Solid Freeform Fabrication 2019: Proceedings of the 30th Annual International Solid Freeform Fabrication Symposium – An Additive Manufacturing Conference
Reviewed Paper

3D PRINTING OF COMPLIANT PASSIVELY ACTUATED 4D STRUCTURES

Dhileep Kumar Jayashankar[1], Sachin Sean Gupta[1], Loo Yi Ning Stella[2], Kenneth Tracy[3]

[1]Research Assistant, [2]Student, [3]Assistant Professor
Digital Manufacturing and Design Centre, Architecture and Sustainable Design Pillar
Singapore University of Technology and Design, Singapore

Abstract

Additive manufacturing has begun to revolutionize the production of various physical technologies that depend on bespoke geometry and tailored material properties for function. This includes the design of compliant mechanisms, which rely on an integral coupling between geometric and material parameters to attain the elastic flexibility necessary to accommodate programmed deformation. While kinetic structures with compliant parts are typically activated by the application of a mechanical force, alternative means of achieving motion are available, such as the use of smart, 4D, or stimuli-responsive materials which react to environmental conditions. In this research, a combination of compliant mechanisms and water-responsive chitosan biopolymers was explored to create flexible, programmable passive actuators, enabled by 3D printing. A set of compliant joints were modeled, simulated, fabricated, and tested to determine the optimal design for use in the actuator. The actuator was then iteratively tested with wetting and drying of chitosan films to invoke a specific shape change, which was analyzed for accuracy, speed, and consistency. The study concluded with a discussion of the implications of synthesizing compliant mechanisms, chitosan biopolymer, and additive manufacturing for next-generation adaptive structures.

Keywords: Compliant Mechanism, Passive Actuation, Additive Manufacturing, Chitosan Biopolymer

Introduction

Compliant mechanisms (CM) leverage the elasticity of their flexible members to achieve motion [1]. This contrasts from traditional mechanisms, which are composed of assemblies of discrete, rigid parts connected at articulating joints. Dependence on material properties rather than mechanical components means that CM offer advantages such as no hysteresis, compactness, ease of fabrication, inherent simplicity, low weight, high reliability, and frictionless and wear-free motion [2]. These benefits indicate the CM can be implemented where typical maintenance for traditional joints becomes problematic. This appears in fields such as biomedical implants, soft robotics, building structures, space research, and engineering at micro- and nanometer scales [3][4]. While offering such appealing advantages, CM nonetheless suffer from design and fabrication issues: conventional manufacturing methods become infeasible for producing a CM with the bespoke geometry that may be required for a specific application. Advanced mechanism technologies are required for realizing novel compliant structures with specially programmed deformation.

With its inherent freedom of geometric complexity and ever-expanding repertoire of materials to suit high-performance applications, additive manufacturing (AM) is poised to revolutionize that production of CM. Products created through AM have rapidly transitioned in the last decade, from their humble beginnings as delicate scale models to novel, direct-use objects and structures with enhanced capabilities [5]. AM is a powerful tool for fabricating next-generation products whose performance requirements depend on both geometric and material parameters, which constitute an inseparable relationship in the case of compliant mechanisms. Mirroring the monolithic nature of compliant mechanisms, AM is reputed for its ability to fabricate objects in one continuous step. Furthermore, AM offers a heightened degree of customizability compared to other manufacturing processes, which in turn enables an expanded design space for CM. CM-AM has only just begun to be seriously investigated in variety of fields, spurred by recent advances in computer-aided design (CAD) and simulation tools. In the realm of soft robotics, Mutlu et al. have printed compliant prosthetic fingers using fused deposition modeling (FDM) of thermoplastic elastomers, following systematic finite element analysis (FEA) of different flexure types [6]. The team demonstrated that a single homogenous elastic material, when designed appropriately, could achieve the desired deflection behavior for the bending finger. Gaynor et al. opted for richer material exploration,

implementing multi-material inkjet printing to create a topologically optimized compliant force inverter [1]. This work proved the ability of AM to physically realize nonstandard CM design solutions, and the utilization of both rigid and soft photopolymers was key to improving the efficiency of the inverter. AM-CM has not only been restricted to polymers. NASA, the American aeronautics and space agency, has even experimented with titanium metal 3D printing using an electron beam melting (EBM) process to create lightweight, expandable parts which do not require lubrication; the authors emphasized that these properties are essential for space exploration [7].

While the research developments mentioned above demonstrate the diversity of AM processes and materials that have been implemented in CM production, the common feature was the use of mechanical force to instigate the motion of the compliant structure. However, alternative sources of energy exist for inducing the compliant motion, which can be useful when mechanical inputs are neither desirable nor possible. Temperature-responsive, photosensitive, and hygroscopic materials have the ability to respond to environmental stimuli such as heat, light, and water, respectively, undergoing a change in physical state (such as shape or mechanical properties) that can be manipulated to achieve target motion. This opens the possibility to create smart, "4D" objects and structures that can transform independently when placed in a certain environment, with change over time representing the fourth dimension [8]. The term 4D printing refers to the direct printing of smart materials, whereas this work pursues an alternative strategy of printing the compliant parts that are later assembled with a smart material (chitosan). Regardless of the approach, such structures are considered passively actuated due to a lack of active input of electrical or mechanical energy, assuming that the environmental stimulus is naturally present during use. This is especially poignant in the use of water as source of movement for passively actuated objects, given the ubiquity of ambient humidity, rain, or bodies of water. Promising research has already been conducted in the pairing of water-responsive materials with additively manufactured CM to create passive 4D objects. Foresterio et al. have demonstrated the use of multilayer wood veneer struts as cellulose-based actuators, joined with FDM-printed compliant polyurethane nodes to construct shape-shifting space frames that responded to variations in humidity [9]. In this case, the compliant nodes acted as bifold hinges that afforded degrees of flexibility to the struts, allowing them to rotate in order to morph into desired global curvatures. Tibbits et al. took a different route, directly printing hygroscopic polymers and nonactive polymers into compliant configurations, resulting in self-evolving structures when immersed in water [10]. These compliant structures took the form of printed assemblies of modules, links, and discs that could stretch or fold by leveraging differences in swelling capabilities to achieve targeted transformation. While the results of both works showed the great potential of merging hygroscopic actuation with CM, limitations in general applicability resulting from slow response time (for the former) and load-bearing ability of the hygroscopic material in question (for both) were observed.

However, alternative materials and compliant structure designs exist that can improve upon the current limitations in strength and speed of hygroscopically actuated compliant structures. So far to the authors' knowledge, the combination of CM with chitosan biopolymer is yet to be explored. Chitosan is a derivative of chitin, the world's second most abundant polymer after cellulose [11]. Chitosan biopolymer has been used in industrial applications ranging from cosmetics, agriculture, textiles, food processing, and tissue engineering. Its extensive applicability stems from an exceptional combination of hygroscopicity, processability, and biodegradability, in addition to its ability to form composites with sound tensile strength [12]. These mechanical properties decrease appreciably when chitosan is exposed to water, causing amplified deformation to the structure to which chitosan is bonded [13]. This transition happens on the order of minutes, enabling rapid changes that can be accommodated by well-designed CM. Considering this potential technological synergy, this work explored the combination of CM and water-responsive chitosan biopolymers to create flexible, programmable passive actuators, enabled by 3D printing. These actuators were afforded flexibility through the use of compliant joints that were designed to achieve a specific global curvature change of the actuator. In this study, different compliant joint designs were designed, modeled, simulated, printed, and tested. A single design was selected that was applied to the nodes of the actuator, which took the form of a truss-inspired cantilever fitted with hygroscopic chitosan films. This actuator was printed using fused deposition modeling (FDM) technology and tested for its motile capabilities in the pursuit of the target curvatures, including the repeatability of the transformation. These results were critiqued, as well as the general effectiveness of the synthesis of CM, chitosan biopolymer, and AM.

Design Methodology

Theory of compliant passive actuator

The theory behind the motion of this passively actuated structure lies in strategic positioning of the chitosan films within the structural assembly. Chitosan, a deacetylated form of chitin extracted from arthropods, is highly hygroscopic in nature and can be manufactured into different forms for engineering and medical applications [11]. In this work, chitosan is reinforced with cotton fiber gauze and formed into thin films. The production of chitosan films involves preparation of chitosan solution, filtering the solution with 50 μm accuracy to remove impurities, degassing the solution to remove air bubbles, and then casting the solution into molds. The films are then dried, neutralized, washed, and dried a second time. Based on measurements from previous work [12], these chitosan films have the ability to extend 12% in length with the absorption of water, thereby serving as a passive actuation mechanism. Furthermore, chitosan films exhibit decreases in their mechanical properties when exposed to water [13]; thus, by having the chitosan films serve as critical tensile members, any loss in properties of the chitosan results in amplified deformation of the actuator. The cantilevering actuator purposefully fails when the chitosan becomes weak, eventually bringing forth a "wet state" configuration of the systems once the chitosan has fully elongated. As the chitosan films dry, they undergo significant internal forces that are sufficient to pull the actuator back upwards toward a "dry state" conformation once all water has evaporated. This operation can proceed in a cyclic manner and has been validated in previous studies using traditional revolute joints using a pin and ball bearing, as seen in Fig. 1. This paper represents progress in attaining specific shape changes that can be programmed by the carefully designed deformation of compliant joints.

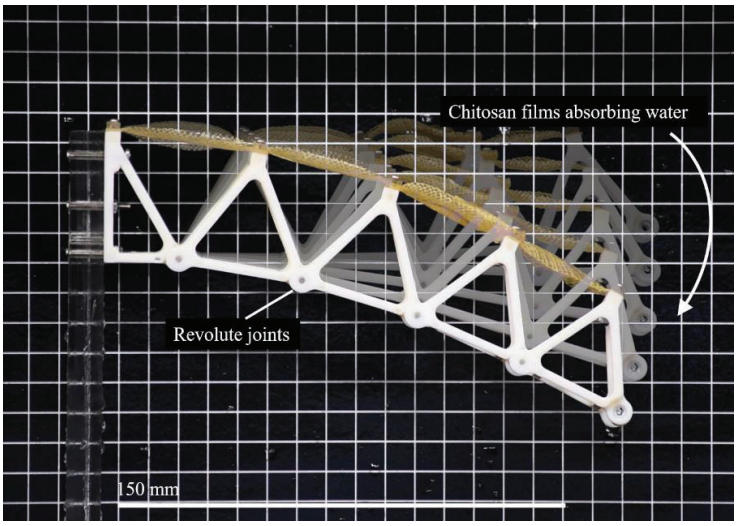

Fig. 1 Previous work of chitosan based passive actuator with revolute joints

Selection of Compliant Flexure Design

In modern manufacturing, advanced mechanism technologies enable design engineers to use the concept of miniaturizing mechanical structures to achieve desired motion through new materials and with their possibilities by creating compliant structures. In this design methodology, a set of CM were explored using finite element methods (FEM) with FDM additive manufacturing technology to replace the conventional revolute joints with flexural hinges for actuator designs. In this early stage of development, as opposed to following the pseudo rigid body approach or the topology optimization method to design the compliant flexure, intuitive physical prototyping was used to create a proof-of-concept. To achieve a planar motion, a primitive type single-axis flexure was designed as a three-node beam element with three degrees of freedom (DOF) per node in different geometrical configurations [2]. Various CM designs (henceforth abbreviated as CMD) were explored in terms of achievable range of motion based on different geometries and identical thickness to find the allowable stress and maximum deflection that were suitable for the structural movement provided by the chitosan film expansion. If

the flexure did not possess sufficient compliance, the movement of the actuator would be impeded. This desired deflection was calculated as the vertical deflection of the most critical flexure between the neutral (partly wet and partly dry) and fully wet state actuator configurations, as shown in Fig. 2. Through measurement of the digital models, it was found that the joint deflection needed to reach 4.15 mm under the self-weight loading of the actuator to enable it to transition from initial state to wet state. The total truss weight in the dry state was estimated to be 20 gm. However, the standard weight of 50 gm which was nearest to the actual loading conditions was chosen to test the joint deflection. Therefore, a minimum threshold deflection under 50 gm was estimated, informed by FEM simulations of the joint deformation. This minimum deflection was coupled with a factor of safety of 1.5 to account for any underestimate in the simulation, resulting in a value of 9.34 mm. Thus, four different flexure designs were digitally and physically tested with 50 gm of weight hanging from their free end to reflect their loading behavior in the actuator. Their vertical deflections were measured and compared to 9.34 mm.

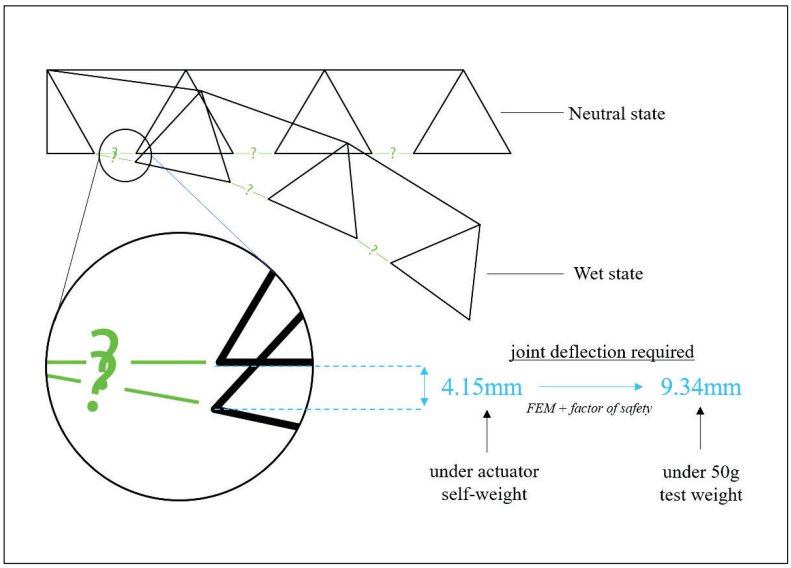

Fig. 2 The flexure must be compliant enough to deflect 9.34 mm under the load from a 50gm test weight in order to achieve the targeted shape change

Four compliant models were designed based on attaining large angular deflection and with a low axis of rotation. The integral component of the CM in the four designs were flexures which allowed controlled bending that counted towards motion. In traditional compliant designs, flexibility is attained along the axis by gradually thinning out material with specific geometry [2]. By assessing several primitives, it was observed at the initial scale of testing that the thinning out of material at one specific area introduces critical level of stress concentrations that eventually increases the overall stress, potentially causing the system to actuate inconsistently or even fail over a period of time after multiple cycles. To counteract this, only an effective design with minimal stress and larger angular deflection of flexure could overcome these challenges to achieve the desired motion in dynamic conditions. A series of flexure designs were conceived considering spring-based mechanisms to allow greater freedom of movement. The springy-derivative design brought two benefits: the load in each flexure could be spread out equally across a series of turns, instead of being constrained to one single area that weakens the structure; and secondly, it could be used to control the structure by defining pre-induced bending in the system. Fig. 3 shows the springy-derivative flexural designs.

Fig. 3 Different springy-derivative flexural designs (a) CMD 1 (b) CMD 2 (c) CMD 3 (d) CMD 4

In addition to degree of motion, strength of the CM must be considered. Strength can be obtained by a load test to determine the force or the stress-deflection involved in the flexure. A static non-linear structural FEM analysis was applied to two-dimensional compliant flexure designs. The four compliant models, two with identical geometry but with different end conditions, and two alternatives, were analyzed by applying a point load of 0.5 N at the right extreme end, considering flexure as a cantilever beam. The material properties of the compliant flexure were an important characteristic to predict the fatigue failure through FEA methods. The properties of Stratasys' ASA material in its XZ direction with a Young's modulus and Poisson's ratio of 2010 MPa and 0.394, respectively were utilized. Fig. 4 shows the maximum stress and maximum deflection of the four compliant mechanism designs. From FEM analysis, CMD 1 and CMD 2 did not possess significant levels of difference in stress with 47.843 MPa and 47.185 MPa, and similarly with deflections of 22.583 mm and 22.064 mm, respectively. CMD 3 and CMD 4 had a marginable difference in stress with 44.172 MPa and 46.189 MPa and deflections of 21.663 mm and 20.147 mm. The results were plotted between maximum stress and maximum deflection, as shown in Fig. 5, in order to find the suitable design which had low stress with high deflection. Out of the four designs, CMD 3 best satisfied the condition from an FEM simulation point of view. These simulation results were complemented with physical load tests of printed CMD.

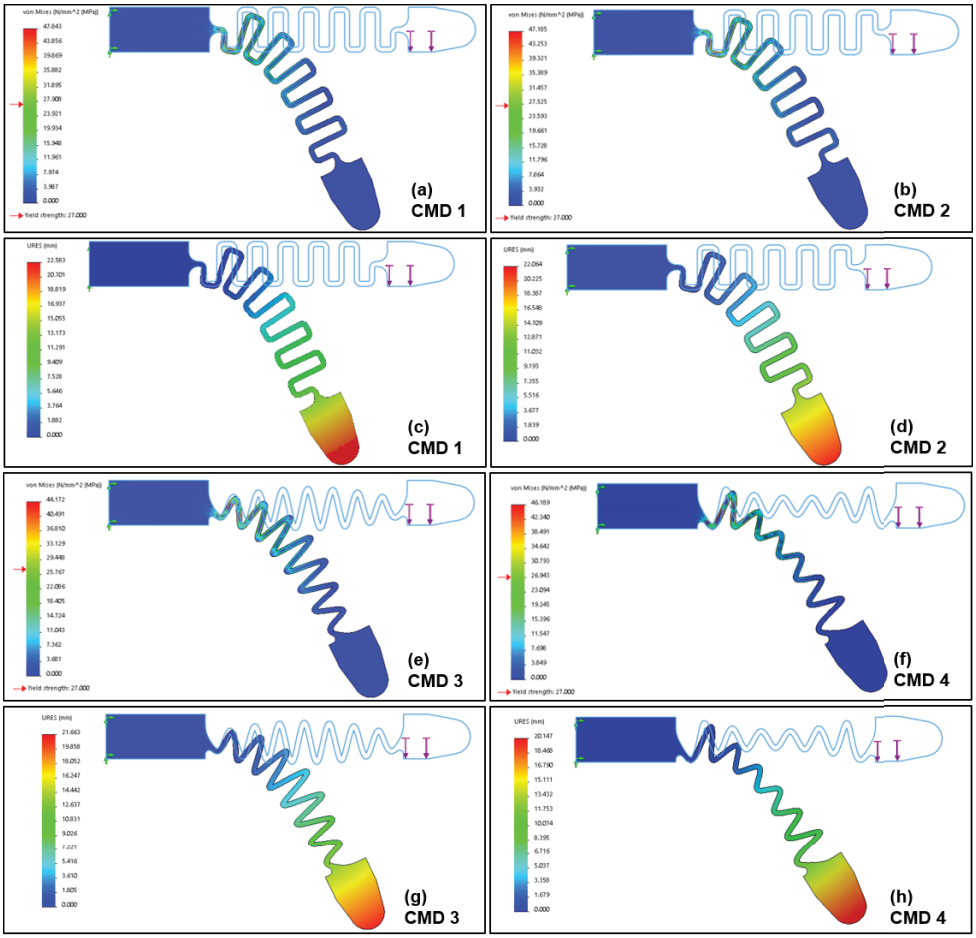

Fig. 4 FEA simulation for four different CM designs (a, b, e & f) Maximum stress (c, d, g & h) Maximum deflection

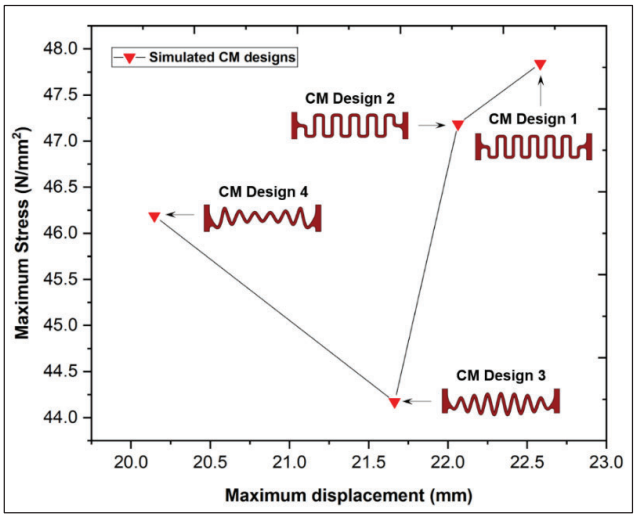

Fig. 5 Maximum stress vs maximum displacement from FEA simulation for four different CM designs

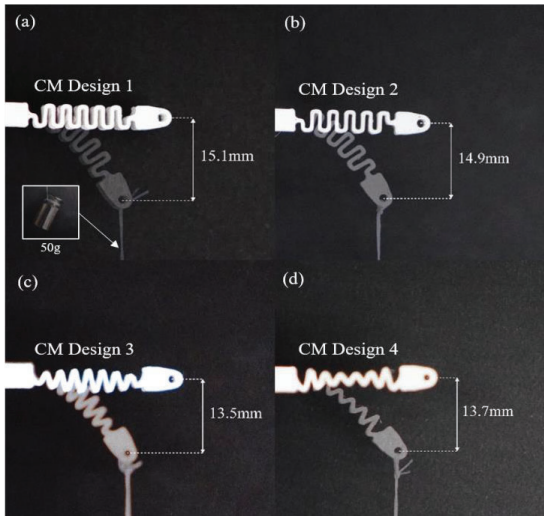

Fig. 6 Flexure test of (a) CM Design 1 (b) CM Design 2 (c) CM Design 3 and (d) CM Design 4. The targeted deformation value was 9.34mm under these load conditions, which all the joints surpassed

For the physical testing, the flexures were 3D printed on the Fortus 450mc machine using ASA material in the XZ direction. Fig. 6 shows the results of these tests. CM Design 1 exhibited the highest deflection (15.1 mm) and CM Design 3 demonstrated the lowest (13.5mm); however, all the joint designs successfully surpassed the minimum compliance needed for the first joint. Thus, to finalize the flexure design, the stress results from the FEM simulation were the primary data used to narrow the selection. As stated above, CM Design 3 was predicted to undergo the least stress between all the designs, and so, CM Design 3 was selected for the actuator. The differences in the deformation results between the FEM simulations and the physical experiments can potentially be attributed to nuances of the AM process. In contrast to conventional manufacturing, AM-produced parts possess different properties in each direction that vary based on the direction of printing. In this case, the CM were printed in the Z direction, which is perpendicular to the applied load, and so in the FEM simulation, only the tensile strength and Poisson's ratio for the Z direction were included. This might have caused differences from the physical behavior. Additionally, because it is supported at only one end in the physical experiment, the CM has greater degrees of freedom to rotate or twist in other axes, which might have decreased the measured vertical displacement. In future studies, flexural strength and a tailored bending theory should be included in FEM to approximate the solution.

Design of compliant structures

The passive actuator assembly was designed as a spatial structure, inspired by the lightness of a space truss. The assembly consists of structural members, CM Design 3 at the nodes, and chitosan films that act as critical tension elements. Through expansion and contraction of the chitosan films mediated by the compliant joints, a desired physical transformation of the structure could be achieved. The cotton-fiber reinforced chitosan film was responsible for the passive actuation due to their responsivity to moisture. A detailed research study about the actuation time for chitosan film was conducted by the authors and recently published [12]. One notable piece of information gained from the work was the use of cotton-fiber reinforcement for improved strength of chitosan film. Additionally, the orientation of the reinforcement plays a vital role by accommodating the films' hygroscopic expansion. As shown in Fig. 7, 0°/90°-oriented films have restricted expansion due to horizontally- and vertically-aligned fibers, whereas 45°-oriented films possess greater expansion due to crisscross lay-up of fiber along their direction of applied force. From the authors' previous work, it was reported that chitosan films with 45° oriented cotton-fiber reinforcement can expand up to 12.8 % linearly along the direction of applied force in a completely wet state (i.e. saturation state) due to hygroscopic swelling. Furthermore, the films yielded an

internal drying force of 19 N during drying in the reverse direction, which is the property enabling lifting of the actuator into its dried conformation.

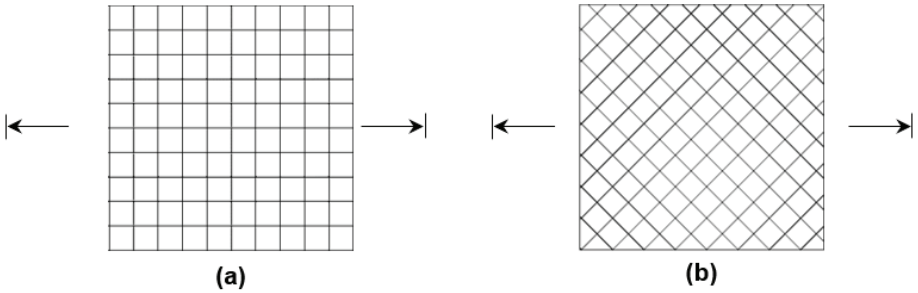

Fig. 7 Orientation of cotton-fiber reinforcement (a) 0°/90° with respect to the applied force (b) 45° with respect to applied force

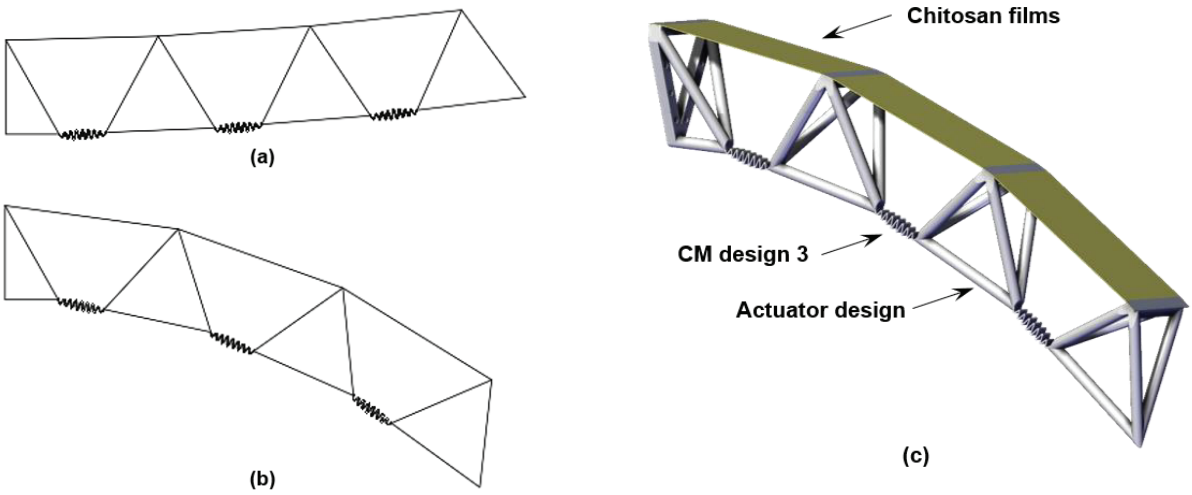

Production of AM parts

The actuator was printed on a Stratasys Fortus 450mc machine, which operates through fused deposition modeling (FDM) printing technology. FDM, one of the most widespread of AM processes, was selected for its ability to create parts of satisfactory strength and durability at low cost. The model of the passive actuator was converted into an .stl file and then imported into Stratasys' Insight software for slicing as shown in Fig. 9 (a). A default layer height of 0.178mm using the T12 nozzle tip was selected, with choice of sparse infill for both the part interior and support material. The material selected for the actuator was ASA, Stratasys' propriety model material that is similar to acrylonitrile butadiene styrene (ABS) in properties. SR30 was selected as the corresponding water-soluble support material, enabling attainment of the future part with minimal post-processing. Upon finalization of the print settings, machine-readable files with toolpath instructions were automatically generated using the Insight software and sent to the printer. The actuator was printed as a single part within 4.5 hours and then placed in a solution bath to remove the support material as seen in Fig. 9 (b). In parallel, enclosure strips for securing the film on the actuator were laser-cut from thin acrylic sheets.

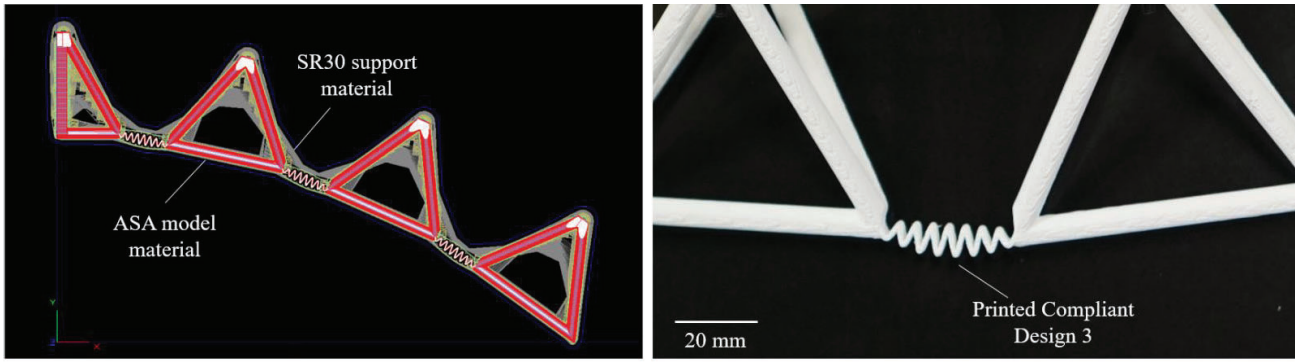

Fig. 9 3D printing of the actuator (a) Sliced model of the actuator before printing (b) Print results of CM Design 3

Assembly and Test Setup

Upon completion of 3D printing and laser-cutting of chitosan films, the various components of the actuator were assembled. The films were sequentially laid upon the actuator, clamped with the acrylic strips, and secured with metal fasteners. The fully realized actuator first assumed a neutral flat conformation as opposed to a curled dried one due to exposure of the film's due ambient humidity. The actuator was mounted to an acrylic mounting surface inside a test setup that was created to interchangeably administer water or dry air to the structure. To test the performance of the compliant actuator, water and air were applied to the films for 20 minutes and 45 minutes, respectively, in a cyclic manner. The motion of the actuator was recorded using videography techniques. Three quantitative parameters, amount, speed, and repeatability of the deformation, were measured by analyzing and superimposing sequence frames from the videos. The physical results were then compared to the designed curvatures to verify the latter's accuracy.

Results and Discussion

Results

In general, the actuator performed well, offering large degrees of deformation with no signs of mechanical failure in any of the films, actuator members, or compliant joints. Fig. 10 (b) shows a superimposed image of the actuator with the films in their fully wet and dry states during one of the testing cycles. This is compared with the targeted design of wet and dry state curvatures as seen in Fig.10 (a). It can be visually observed that while the general shape change was achieved, there was still significant variations from the expected results. To quantify the degree of shape change of the physical experiment the deflections of the actuator were calculated. Variable

deflection of the joint was expected considering that the loading conditions of the joints differed depending upon their location along the cantilever length. However, the stretching, compression, and bending of each joint was too small to accurately measure based solely on the images, and so only the deformation of the entire actuator was measured. Further steps could be taken in future work to find a reliable means of measuring the joint deflection.

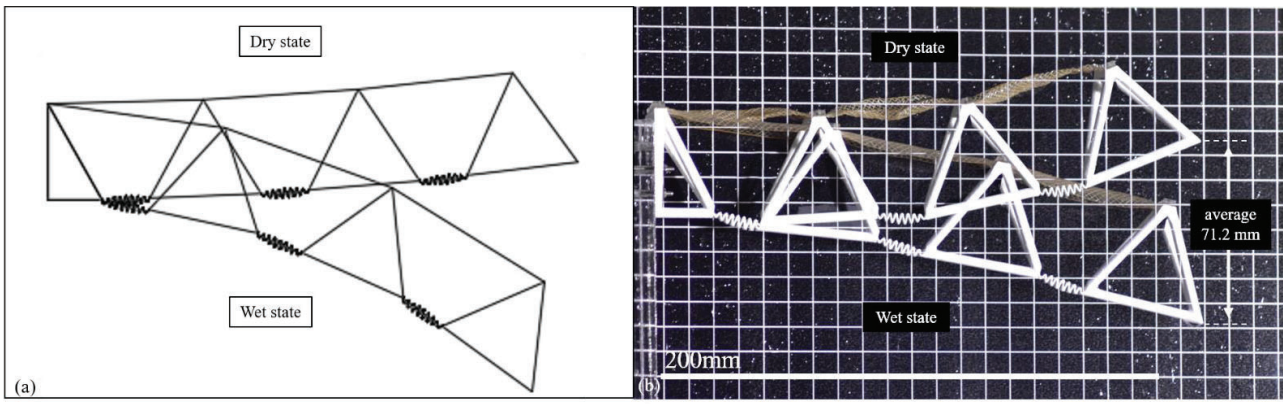

Fig. 10 Comparison of (a) Simulated curve of dry and wet state (b) Physical results of dry and wet state curvature

The average total deformation between the two states of the actuator was calculated to be 71.2mm, measured by changes in height of the cantilevering end of the actuator. This 71.2 mm represents nearly one-third of the total actuator length, which points to the ability of the CM to accommodate a relatively large range of motion. The expected deformation from 2D simulation was 95.6mm, and so evidently the chitosan did not expand to their 12.8 % capacity as expected. It was hypothesized that this was not due to inadequate joint compliance, as the joints already showed much potential for elastic deformation. It is possible that even though the films lose much of their stiffness when saturated, that there was still insufficient driving force to cause significant mechanical strain of the films. One potential workaround would be to implement another tensile element to the assembly that, when added on top of the assembly's self-weight, could encourage the full elongation of the chitosan films. To determine the actuation time, the video documentation was analyzed to determine at which times the actuators ceased to show discernible changes in curvature during the 20-minute-wetting and 45-minute-drying windows. The time for full actuation from the dry to the wet state averaged on 12.2 minutes, while the reverse process lasted on average 44.2 minutes. The faster response time for achieving the wet state was expected due to chitosan's hydrophilic tendencies. In each testing iteration, the chitosan films (combined weight of 2.75 gm) successfully lifted the actuator's weight (total weight of 13.5 gm), proving that the films could bear at several times their own weight during drying.

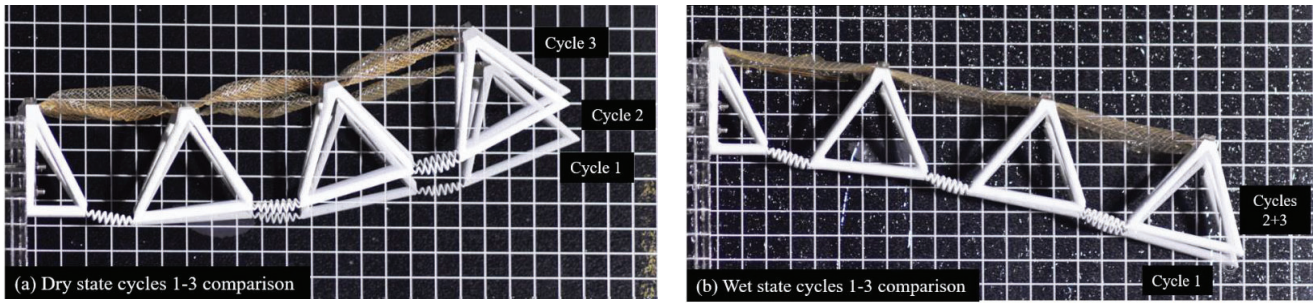

Fig. 11 Comparison of curvature over three cycles (a) Dry state (b) Wet state

Fig. 11 (a, b) reveals the dry states and wet states for the three testing cycles to understand the repeatability of the shape change. It is clear that the wet state showed excellent consistency among the various experiments, with no distinction in shape seen in cycles 2 and 3. The dry state, however, possessed some variation, which could possibly be due to uneven drying. It is also wondered if the chitosan film's drying ability features some slight

a stepwise sequence of motion of the actuator as it transitioned from dry to wet states was not developed. A robust simulation should be developed, as well as an improved means of measuring the shape changes through technologies such as 3D scanning or motion tracking to accurately compare to the simulation. Finally, while the 3D printed parts were strong enough to handle the loads for this phase of experimentation, the actuator design would need to be substantiated in order to seriously consider this class of actuator for structural applications. Otherwise, a different 3D printer, material, and/or printing process could be selected, as these decisions presently stemmed from factors of cost and availability.

Foreseeable future work lies in scaling up this prototype with tests in real-world environmental conditions, gauging its effectiveness as a 4D compliant structural object. New applications should be conceived, such as developing these structures for rain-responsive shelters or infrastructure. Because the speed of actuation depends on the rate of water absorption by the films, fast-acting movement is possible for climates that experience large amounts of sudden rainfall, such as the tropics. Regions with high amount of relative humidity for sustained periods will also serve to actuate the potential structures to their full capacity, albeit more slowly. However, before long-term outdoor exposure can be considered, the ability of chitosan to survive the onslaught of heat and decomposing microorganisms must be improved with environmental degradation studies. These material science developments should come coupled with AM advancements, which together can hopefully one day enable the creation of fully 3D printed, adaptive biomaterial structures.

Acknowledgements

The authors would like to thank many institutions affiliated with the Singapore University of Technology & Design, including the Fermat Lab, Digital Manufacturing & Design Research Center (DManD), the SUTD-MIT International Design Center (IDC), Architecture & Sustainable Design Pillar (ASD), and the Fabrication Laboratory.

References

[1] A. T. Gaynor, N. A. Meisel, C. B. Williams, and J. K. Guest, "Multiple-Material Topology Optimization of Compliant Mechanisms Created Via PolyJet Three-Dimensional Printing," *J. Manuf. Sci. Eng.*, vol. 136, no. 6, p. 061015, 2014.

[2] N. Lobontiu, *Comliant Mechanism: Design of Flexure Hinges*. 2002.

[3] V. Parenti-Castelli and N. Sancisi, *Synthesis of Spatial Mechanisms to Model Human Joints*. 2013.

[4] A. Körner *et al.*, "Flectofold - A biomimetic compliant shading device for complex free form facades," *Smart Mater. Struct.*, 2018.

[5] T. D. Ngo, A. Kashani, G. Imbalzano, K. T. Q. Nguyen, and D. Hui, "Additive manufacturing (3D printing): A review of materials, methods, applications and challenges," *Compos. Part B Eng.*, vol. 143, no. December 2017, pp. 172–196, 2018.

[6] R. Mutlu, G. Alici, M. In Het Panhuis, and G. Spinks, "Effect of flexure hinge type on a 3D printed fully compliant prosthetic finger," *IEEE/ASME Int. Conf. Adv. Intell. Mechatronics, AIM*, vol. 2015-Augus, pp. 790–795, 2015.

[7] E. G. Merriam, J. E. Jones, and L. L. Howell, "Design of 3D-Printed Titanium Compliant Mechanisms," *Proc. 42nd Aerosp. Mech. Symp.*, pp. 169–174, 2014.

[8] Z. X. Khoo *et al.*, "3D printing of smart materials: A review on recent progresses in 4D printing," *Virtual Phys. Prototyp.*, vol. 10, no. 3, pp. 103–122, 2015.

[9] F. Forestiero, N. Xenos, D. Wood, and E. Baharlou, "Low-tech Shape-Shifting Space Frames," 2018.

[10] D. Raviv *et al.*, "Active printed materials for complex self-evolving deformations," *Sci. Rep.*, 2014.

[11] P. K. Dutta, J. Duta, and V. S. Tripathi, "Chitin and Chitosan: Chemistry, properties and applications," *J. Sci. Ind. Res. (India).*, vol. 63, no. 1, pp. 20–31, 2004.

[12] Sachin Sean Gupta, Dhileep Kumar Jayashankar, Naesh D Sanandiya, Javier G. Fernandez, Kenneth Tracy "Prototyping of chitosan-based shape-changing structures," vol. 2, pp. 441–450, 2019.

[13] S. Alvarado, G. Sandoval, I. Palos, S. Tellez, Y. Aguirre-Loredo, and G. Velazquez, "The effect of

relative humidity on tensile strength and water vapor permeability in chitosan, fish gelatin and transglutaminase edible films," *Food Sci. Technol.*, vol. 35, no. 4, pp. 690–695, Oct. 2015.
[14] I. Q. Meng, "A design method for flexure-based compliant mechanisms on the basis of stiffness and stress characteristic," pp. 1–110, 2012.
[15] N. Lobontiu, J. S. N. Paine, E. Garcia, and M. Goldfarb, "Design of symmetric conic-section flexure hinges based on closed-form compliance equations."
[16] Sebastian Linss and Andrija P. Milojevi and Lena Zentner, "Considering the design of the flexure hinge contour for the synthesis of compliant linkage mechanisms," in *58th Ilmenau Scientific Colloquim*, 2014.